Interperiod Correlation Model for Mexican Interface Earthquakes

Miguel A. Jaimes[a)] **and Gabriel Candia,**[b),c)] **M.EERI**

This article presents a correlation model for pseudo-acceleration, peak ground acceleration, and peak ground velocity residuals using a database of Mexican subduction interface earthquakes at rock sites (NEHRP Class B). A mixed-effect regression model, a ground motion model, and 40 event recordings (418 records) with moment magnitude between five and eight were used to develop a magnitude-independent correlation model. This region-specific model yields consistently higher correlation values compared with similar studies developed for shallow crustal regions and other subduction zones worldwide, particularly for pseudo-acceleration values at distant periods. These results support the idea of using a region-specific and mechanism-specific correlation model for Mexico's subduction zone. [DOI: 10.1193/080918EQS200M]

INTRODUCTION

The aim of a correlation model between total pseudo-acceleration residuals at different structural periods is to define the joint distribution of pseudo-acceleration (*Sa*) values and carry out (1) a vector-valued probabilistic seismic hazard analysis (Baker and Cornell 2006; Goda and Atkinson 2009); (2) the construction of conditional mean spectrum, which accounts for the (empirical) statistical dependence between spectral ordinates (e.g., Baker and Cornell 2006, Carlton and Abrahamson 2014, Cimellaro 2013, Lin et al. 2013, Daneshvar et al. 2015); (3) a simulation of response spectra given an earthquake scenario (Baker and Cornell 2006); and (4) a seismic risk assessment of interdependent infrastructure (e.g., Inoue and Cornell 1990, Cordova et al. 2001).

In the early work by Inoue and Cornell (1990), a correlation model between spectral velocity residuals in the period range of 0.1 to 4 sec. was developed using the Joyner and Boore (1982) ground motion model (GMM) and 64 records from 12 shallow crustal earthquakes in Western United States. Cordova et al. (2001) computed correlation values for two *Sa* values to improve on the collapse prediction of structures based on inelastic time-history analyses. Later, Baker and Cornell (2006) developed a simplified analytical model for correlation between *Sa* residuals for multicomponent ground motions (e.g., cases with differing periods but the same orientation, cases with differing periods and differing orientations) because of shallow crustal earthquakes. This study used a total of 469 records from 31 earthquakes and the

[a)] Instituto de Ingeniería, Universidad Nacional Autónoma de México, Coordinación de Ingeniería Estructural, Circuito Interior, Ciudad Universitaria, Del Coyoacán, C.P. 04510, Ciudad de México, México; Email: mjaimest@iingen.unam.mx (M. A. J.)
[b)] Facultad de Ingeniería Civil, Universidad del Desarrollo, Av. Plaza 680 Las Condes, Santiago, Chile
[c)] National Research Center for Integrated Natural Disaster Management (CIGIDEN) CONICYT/FONDAP/15110017, Santiago, Chile

Abrahamson and Silva (1997) GMM in the period range of 0.05 to 5 sec. Likewise, Goda and Atkinson (2009) developed an interperiod correlation model over the period range of 0.1 to 5 sec. using the Japanese K-NET and KiK-net strong-motion networks.

Baker and Jayaram (2008) developed an equation for *Sa* correlations using the Next Generation Attenuation (NGA) ground motion library (i.e., shallow crustal earthquakes and within the period range of 0.01 to 10 sec.). This study considered four GMMs (Abrahamson and Silva 2008, Chiou and Youngs 2008, Campbell and Bozorgnia 2008, Boore and Atkinson 2008) and concluded that for periods less than 5 sec., the correlation values were similar among models, whereas important differences were observed if one period was significantly larger than 5 sec. and the other period was significantly smaller than 5 sec.

Jayaram et al. (2011) computed $Sa(T)$ correlations for shallow crustal, subduction slab, and Japanese subduction interface earthquakes using 2,819 ground motions from the K-NET database and the Kanno et al. (2006) GMM for the period range of 0.05 to 5 sec. Interestingly, they noticed an influence of the earthquake source zones and earthquake mechanisms in the computed correlations, which may be due to differences in the average frequency content of ground motions and the goodness of fit of the underlying GMMs. However, they concluded that earthquake magnitude and distance did not affect the spectral correlations significantly. Daneshvar et al. (2015) presented an interperiod correlation model over the range of 0.01 to 5 sec. using 108 horizontal accelerograms from eight earthquakes recorded in Eastern Canada, a region with low-to-moderate seismic activity. They showed that period correlations are more sensitive to magnitude than distance. Furthermore, the authors revealed that the correlation coefficients for Eastern Canada were higher than the Baker and Jayaram (2008) predictions for shallow crustal earthquakes. Ji et al. (2017) presented correlation coefficients based on Chinese earthquake records from 2007 to 2014 (authors did not indicate tectonic environment and type of earthquakes) and the Huo (1989) GMM for a period range between 0.01 and 2 sec. Kotha et al. (2017) developed correlation coefficient predictions for Europe and Middle Eastern regions using about 6,000 ground motions from the Reference database for seismic ground-motion prediction in Europe (RESORCE) database and the Bindi et al. (2014) GMM for the period range between 0.02 and 4 sec. They observed a significant magnitude dependence in the correlation of between-event residuals and that the near-source event- and site-corrected residual correlations are region dependent.

Overall, with the exception of the studies by Jayaram et al. (2011) and Abrahamson et al. (2016), the existing literature on ground motion correlations in subduction zones is scarce, in part because strong-motion databases outside Japan have grown slowly. In addition, several questions remain unanswered; for instance, what are the physical driving factors in a correlation structure, or what is the influence of using global earthquake catalogs versus region-specific catalogs in the correlation models? Therefore, the main objective of this study is to develop a simplified correlation model between *Sa* residuals at rock sites using Mexican interface earthquakes and compare this model to existing correlation models from other subduction zones and tectonic regimes.

STRONG-MOTION DATABASE

This study uses a selection of 418 records from the National Seismological Service (SSN) strong-motion catalog and the Engineering Institute of the National Autonomous University of Mexico (UNAM) compiled by García (2006). These ground motions correspond to

40 interface subduction earthquakes with magnitudes $5 \leq Mw \leq 8$, site-to-source distance $17 < Rrup < 400$ km, and focal depth $9 < H < 29$ km, and they are recorded on 56 free-field rock sites classified as NEHRP Sites Class B (Building Seismic Safety Council 2004) as per García et al. (2005) and García (2006). A summary of the selected earthquakes is shown in online Appendix Table A1. In addition, Figure 1 shows the location of epicenters and the location of recording stations.

The magnitude and rupture distance distribution of the 418 selected records is shown in Figure 2. Notice that this data set has a large number of records with magnitude $Mw \leq 6$

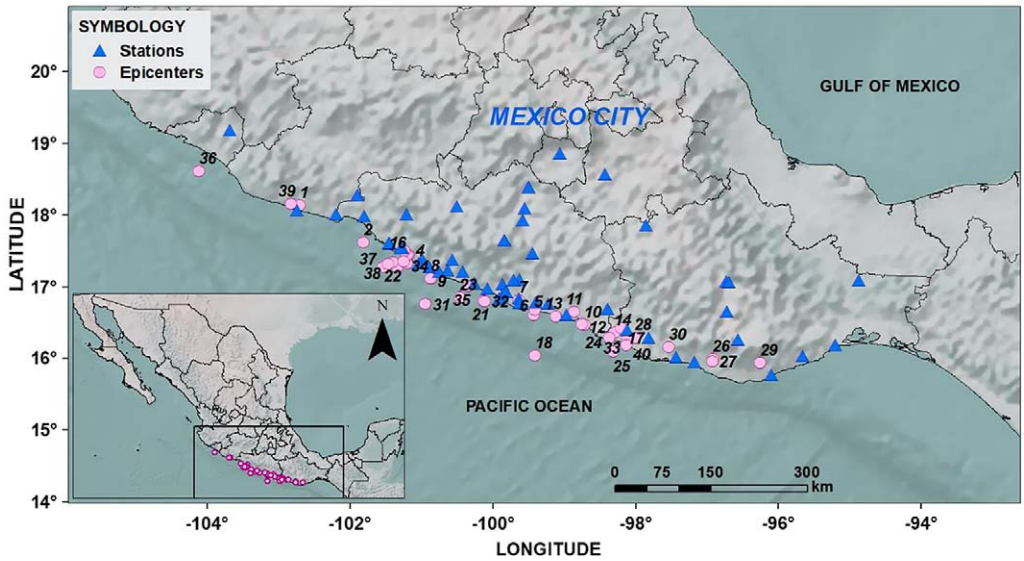

Figure 1. Map of Mexico showing epicenters of interface earthquakes analyzed in this study. Each event is identified by a number, which is keyed to online Appendix Table A1. Recording stations are shown with triangles. Inset: Location of region of the considered earthquakes in the Pacific Coast of Mexico. The map was created using ArcGIS version 9.3.

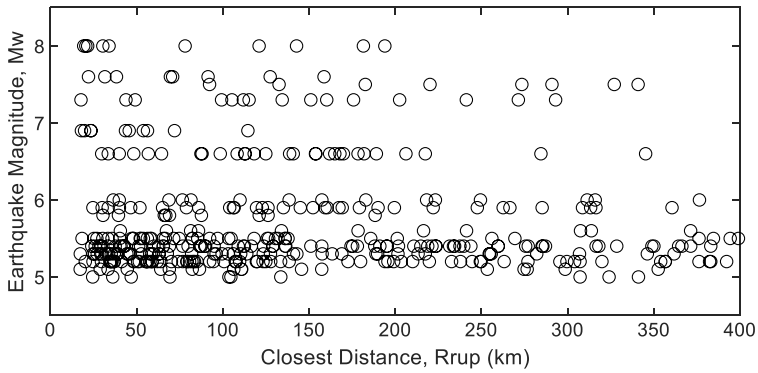

Figure 2. Magnitude-distance distribution of Mexican free-field records used in the model.

at short and large distances but relatively few earthquakes with Mw > 6 at large distances, partly because of insufficient network coverage (García 2006). Initially, we hypothesized that ground motion correlations in this database were magnitude dependent; however, the influence of earthquake magnitude was not significant. Therefore, the correlation analyses presented next are valid for the magnitude range $5 \leq \text{Mw} \leq 8$.

DATA PROCESSING AND ANALYSIS

PROCESSING OF STRONG-MOTION DATA

All acceleration records were processed by applying a baseline correction (Boore 2005) and a high-pass filter with a corner frequency of 0.05 Hz for events with Mw > 6.5 and 0.1 Hz for events with Mw ≤ 6.5 (García et al. 2005, García 2006, Arroyo et al. 2010, Hong et al. 2010, García-Soto et al. 2012, García-Soto and Jaimes 2017). Estimates for the quadratic mean of the peak ground velocity (PGV), peak ground acceleration (PGA), and 5% damped horizontal *Sa* values were computed using the García-Soto and Jaimes (2017) GMM, which has the form given in Equation 1. In this model, ln y_{ij} is the natural logarithm of the observed intensity at site j due to earthquake i, $f(M_i, R_{ij}, \theta)$ is the median intensity at site j due to an earthquake with magnitude M_i at distance R_{ij} and site parameters θ, and the error term δ is a random variable describing the total ground motion variability. As shown in Equation 2, δ is split into a between-event residual δB (i.e., a random effect representing the error component that varies from earthquake to earthquake) and a within-event residual δW (i.e., the error component that varies from site to site):

$$\ln y_{ij} = f(M_i, R_{ij}, \theta) + \delta \tag{1}$$

$$\delta = \delta B_i + \delta W_{ij} \tag{2}$$

The error terms δB_i and δW_{ij} are normal random variables with zero-mean and standard deviation τ and ϕ, respectively. The between-event and within-event residuals δB_i and δW_{ij} were obtained using a mixed-effect regression model (Abrahamson and Youngs 1992, Al Atik et al. 2010). Because δB_i and δW_{ij} are uncorrelated, the standard deviation of the total error is simply $\sigma = \sqrt{\tau^2 + \phi^2}$. For pseudo-accelerations $Sa(T)$, values for τ, ϕ, and σ as a function of period are shown in Figure 3; for PGV, $\phi = 0.58$, $\tau = 0.29$, and $\sigma = 0.65$; and for PGA $\phi = 0.62$, $\tau = 0.38$, and $\sigma = 0.73$. Notice that total variability of $Sa(T)$ values is relatively high but consistent to similar studies, ranging between 0.6 and 0.83.

CORRELATION ANALYSIS

The correlation between the total residuals of two ground motion intensities, say $IM1$ and $IM2$, takes the form of Equation 3 (Carlton and Abrahamson 2014, Stafford 2017):

$$\rho_t = \frac{\tau_{IM1} \cdot \tau_{IM2}}{\sigma_{IM1} \cdot \sigma_{IM2}} \cdot \rho_B + \frac{\phi_{IM1} \cdot \phi_{IM2}}{\sigma_{IM1} \cdot \sigma_{IM2}} \cdot \rho_W \tag{3}$$

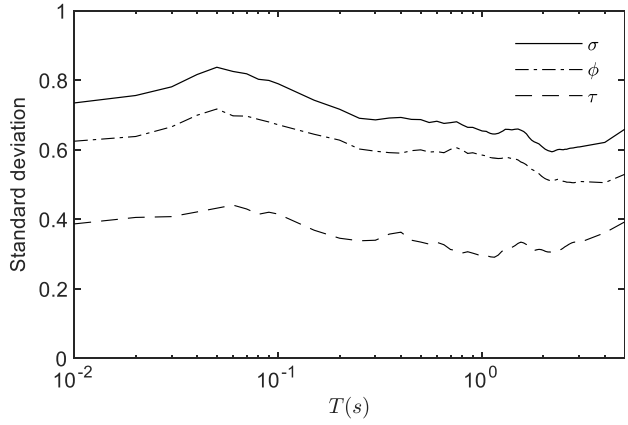

Figure 3. Standard deviations of total residuals σ, between-event residuals ϕ, and within-event residuals τ for pseudo-accelerations $Sa(T)$.

where ρ_B and ρ_W are the correlations of between- and within-event residuals, respectively. For a data set consisting of n ground motions (i.e., $n = 418$ in the current study), ρ_B and ρ_W are computed using the maximum likelihood estimator proposed in Kutner et al. (2004) as:

$$\rho_B = \frac{\sum_{i=1}^{n}\left(\delta B_{IM1}^{i} - \overline{\delta B_{IM1}}\right)\left(\delta B_{IM2}^{i} - \overline{\delta B_{IM2}}\right)}{\sqrt{\sum_{i=1}^{n}\left(\delta B_{IM1}^{i} - \overline{\delta B_{IM1}}\right)^2 \cdot \sum_{i=1}^{n}\left(\delta B_{IM2}^{i} - \overline{\delta B_{IM2}}\right)^2}} \tag{4}$$

$$\rho_W = \frac{\sum_{i=1}^{n}\left(\delta W_{IM1}^{i} - \overline{\delta W_{IM1}}\right)\left(\delta W_{IM2}^{i} - \overline{\delta W_{IM2}}\right)}{\sqrt{\sum_{i=1}^{n}\left(\delta W_{IM1}^{i} - \overline{\delta W_{IM1}}\right)^2 \cdot \sum_{i=1}^{n}\left(\delta W_{IM2}^{i} - \overline{\delta W_{IM2}}\right)^2}} \tag{5}$$

where $(\delta B_{IM1}^{i}, \delta W_{IM1}^{i})$ and $(\delta B_{IM2}^{i}, \delta W_{IM2}^{i})$ are the residuals for $IM1$ and $IM2$ in the i-th ground motion, and $(\overline{\delta B_{IM1}}, \overline{\delta W_{IM1}})$ and $(\overline{\delta B_{IM2}}, \overline{\delta W_{IM2}})$ are their respective mean values computed over the entire ground motion data set.

To illustrate this concept, Figure 4a shows the 5% damped response spectrum recorded at station CALE (Caleta de Campos) during the Mw 8.0 Michoacán earthquake of 19 September 1985; also, the mean and the mean ± one standard deviation response spectra as predicted by Garcia-Soto and Jaimes (2017) are shown in Figure 4. For $IM1 = Sa\,(T = 0.5\text{s})$ and $IM2 = Sa\,(T = 1.0\text{s})$, Equation 2 yields $\delta_{IM1} = \delta B_{IM1} + \delta W_{IM1} = -0.07 - 0.59 = -0.66$ and $\delta_{IM2} = \delta B_{IM2} + \delta W_{IM2} = -0.07 - 0.44 = -0.51$; in other words, the observed $IM1$ and $IM2$ values are, respectively, 0.67 and 0.51 standard deviations below the mean estimates. Repeating this analysis for all the records in the strong-motion database described previously,

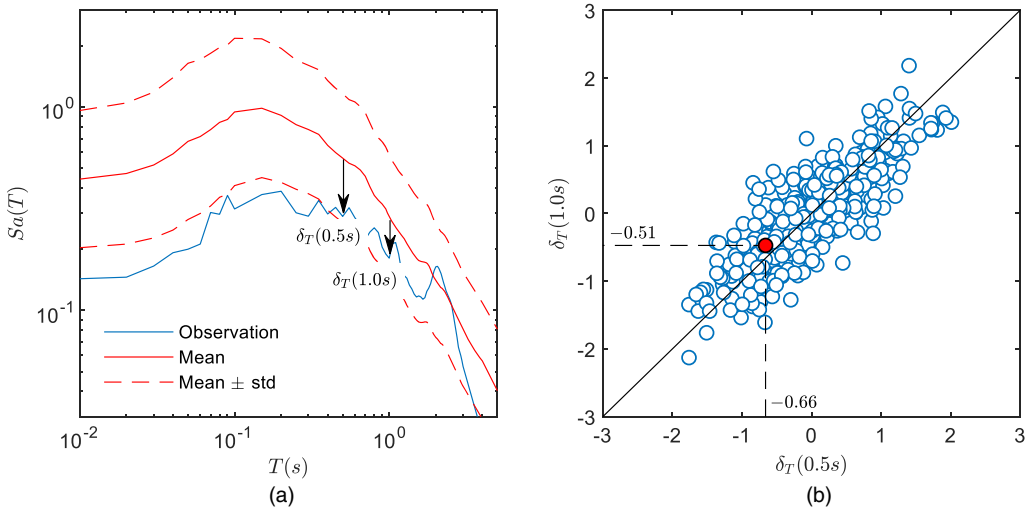

Figure 4. Illustration of the total residuals at station CALE. (a) Predicted and observed response spectrum for the Mw 8 earthquake of 19 September 1985; arrows show the total residuals at $T = 0.5$ sec. and $T = 1$ sec. (b) Total residuals at $T = 0.5$ sec. and $T = 1$ sec. for a set of 418 ground motions.

the scatter plot in Figure 4b depicts the relationship between the total $IM1$ and $IM2$ residuals. From Equation 3, the correlation coefficient is $\rho_t = 0.82$, implying that the knowledge of $IM1$ provides meaningful information about $IM2$.

The empirical correlation between PGA, PGV, and $Sa(T)$ pairs was conducted using the Mexican Strong Motion Database and the García-Soto and Jaimes (2017) GMM. The correlations computed from Equations 3–5 for total pseudo-acceleration residuals are shown in Figure 5. Because ϕs are much larger than τs, it is verified that total and within-event correlations are very similar. For most practical purposes, these differences are not significant. A summary of the correlation coefficients computed with Equations 3–5 is presented in the online Appendix Tables A2–A4. In the strict sense, these coefficients are valid for the quadratic mean of Sa, PGA, and PGV values from the two horizontal-orthogonal components; however, the use of orientation-independent measures of ground motions (e.g., GMRotD50 or GMRotI50, as defined in Boore et al. 2006) leads to similar results. This implies that correlations of Sa values are generally independent of the method used to define a ground motion's Sa (Baker and Jayaram 2008, Baker and Bradley 2017).

As an alternative to the "exact" online Appendix Table A2 (e.g., total correlation coefficients for Mexican interface earthquakes), a continuous functional form with "approximate" values is provided here. A Fourier expansion was used to approximate the correlation between PGV and $Sa(T)$ residuals; the functional form was defined as:

$$\rho(PGV, Sa(T)) = \tanh(a_0 + a_1 \cos a_3 p + a_2 \sin a_3 p) \tag{6}$$

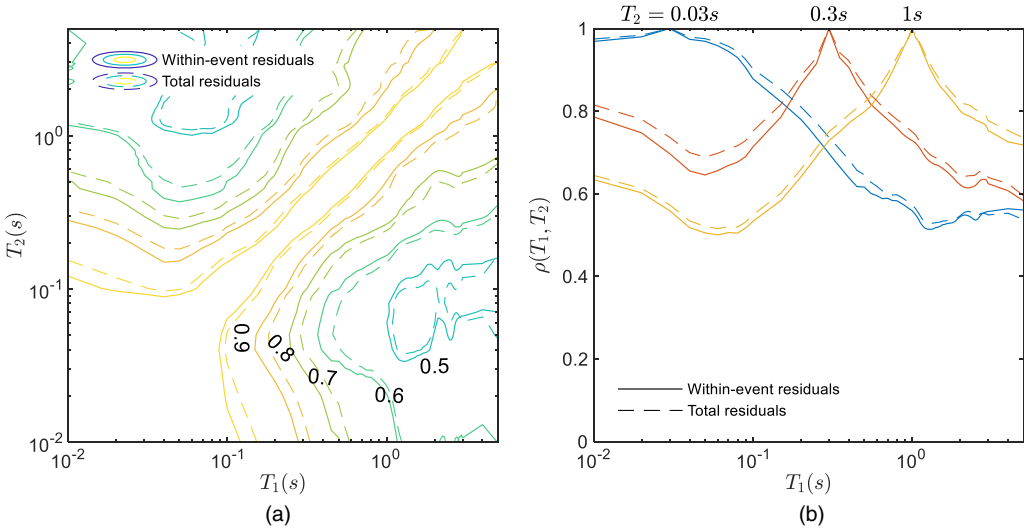

Figure 5. Correlation coefficients for within-event residuals ρ_W (online Appendix Table A3) and total residuals ρ_t (online Appendix Table A2) for (a) periods T_1 and T_2 between 0.01 and 5 sec. and (b) three different T values, $T = 0.03$, 0.3, and 1 sec.

where $\tanh(\cdot)$ is the hyperbolic tangent function, and $p = \log_{10}T$, with 0.01 sec. $\leq T \leq$ 5 sec. Likewise, the functional form proposed by Baker and Jayaram (2008) was used to approximate the interperiod correlations. The latter predictive equation can be written as:

$$\rho(Sa(T_1), Sa(T_2)) = \begin{cases} C_2 & if \quad T_{max} < a \\ C_1 & if \quad T_{min} > a \\ min\left(C_2, C_4\right) & if \quad T_{max} < 0.2 \\ C_4 & if \quad T_{max} \geq 0.2 \end{cases} \tag{7}$$

where $T_{min} = \min(T_1, T_2)$ and $T_{max} = \max(T_1, T_2)$. The period-dependent constants C_1, C_2, C_3, and C_4 are defined by the following:

$$C_1 = 1 - cos\left(\frac{\pi}{2} - b \ln\frac{T_{max}}{max(T_{min}, a)}\right) \tag{8}$$

$$C_2 = \begin{cases} 1 - c\left(1 - \frac{1}{1+exp(100T_{max}-5)}\right)\left(\frac{T_{max}-T_{min}}{T_{max}-0.0099}\right) & if \quad T_{max} < 0.2 \\ 0 & if \quad T_{max} \geq 0.2 \end{cases} \tag{9}$$

$$C_3 = \begin{cases} C_2 & if \quad T_{max} < a \\ C_1 & if \quad T_{max} \geq a \end{cases} \tag{10}$$

$$C_4 = C_1 + d\left(\sqrt{C_3} - C_3\right)\left(1 + cos\left(\frac{\pi T_{min}}{a}\right)\right) \tag{11}$$

Table 1. Regression coefficients used in Equations 6–11

Parameter	PGV model	Parameter	*Sa* model
a_0	1.137	a	0.084
a_1	0.144	b	0.214
a_2	–0.082	c	0.108
a_3	3.069	d	0.418

The parameters a_0–a_3 in Equation 6 and the parameters a–d in Equations 7–11 were determined through a standard nonlinear least-square regression in conjunction with the "variance stabilizing" Fisher transformation of the residuals (Kutner et al. 2004, Baker and Jayaram 2008). The resulting coefficients are summarized in Table 1.

RESULTS AND DISCUSSION

CONTOURS OF EMPIRICAL CORRELATION COEFFICIENTS

Figure 6 shows contours of *Sa* correlation as a function of T_1 and T_2 computed from Equation 3 (values in online Appendix Table A2) and the approximation of Equations 7–11. It is apparent that the analytical model is in very good agreement with empirical values; the standard error of this approximation does not exceed 13%, and we consider that this difference is acceptable. From online Appendix Table A2, it is also apparent

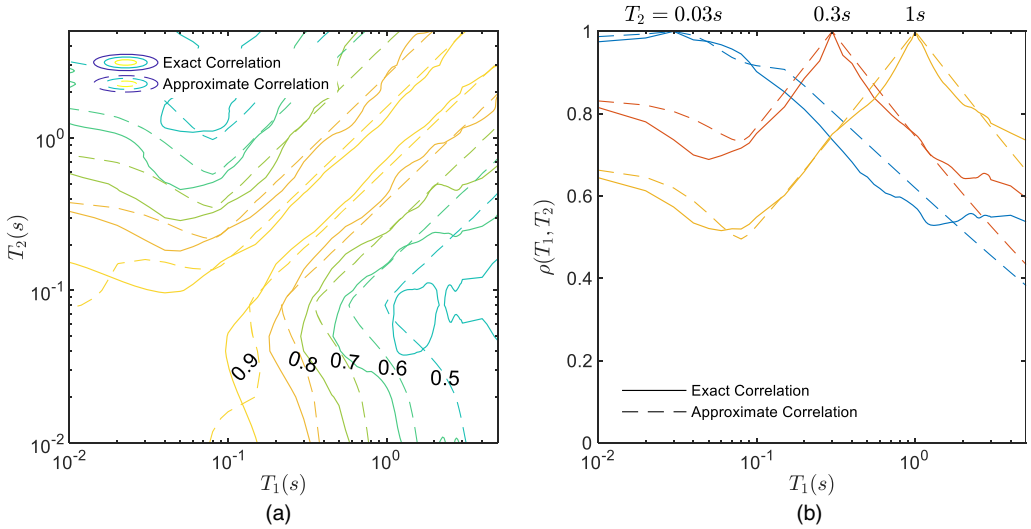

Figure 6. Comparison between "exact" correlations (online Appendix Table A2) and approximate correlations (Equations 7–11) for (a) periods T_1 and T_2 between 0.01 and 5 sec. and (b) T_1 between 0.01 and 5 sec. and $T_2 = 0.03$, 0.3, and 1 sec.

that the correlation between PGA and $Sa(T)$ residuals decreases as the structural period increases. Likewise, values of correlation between PGV and $Sa(T)$ residuals remain almost constant for all structural periods, with an average value of 0.81.

COMPARISON WITH OTHER STUDIES WORLDWIDE

Other than Jayaram et al. (2011) and Abrahamson et al. (2016), very few studies have addressed the problem of interperiod correlations in subduction zones. The correlation model for Mexican subduction earthquakes is compared with three existing models (Baker and Jayaram 2008, Jayaram et al. 2011, Abrahamson et al. 2016), and the results are presented in Figures 7 and 8 in terms of $\rho(T_1,T_2)$, with 0.01 sec. $\leq T_1 \leq 5$ sec. and $T_2 = 0.05$ sec., 0.1 sec., 0.2 sec., 0.5 sec., 2 sec., and 5 sec. In the current study, a shaded region was added to each correlation curve depicting the mean $\pm$ one standard deviation (σ), where $\sigma = (1-\rho^2)(n-1)^{-0.5}$ (Kotha et al. 2017), and n is the number of ground motions in the data set.

From Figure 7 it is apparent that correlation values from Baker and Jayaram 2008 (i.e., shallow crustal earthquakes) are significantly lower than correlations derived from Mexican interface earthquakes. Carlton and Abrahamson (2014) and Kotha et al. (2017) suggest that correlation values are sensitive to the high-frequency content of ground motion records. Therefore, the differences shown in Figure 7 might be attributed to the frequency content of the seed ground motions and the tectonic regime. Also, although the site class imprints no systematic variations in *IM* correlations (e.g., as concluded by Baker and Bradley using the NGA-West 2 database), it should be noted that the current study includes only NEHRP Class B sites, while Baker and Jayaram (2008) used heterogeneous site classes.

Likewise, Figure 8 compares the correlation model for Mexican interface earthquakes with those obtained by Jayaram et al. (2011) for Japan and Abrahamson et al. (2016), who used a global data set but largely dominated by earthquakes from Japan and Taiwan. Figure 8 shows consistent trends among the three models but much larger correlations when T_1 and T_2 depart from each other. Beyond the earthquake's stress drop and the frequency content ground motion correlations (e.g., Kotha et al. 2017), we cannot yet provide a physics-based explanation for it and attribute this difference to a regional effect.

These results support the use of a region-specific and mechanism-specific correlation model for Mexico's subduction zone. This idea contrasts with the observations by Carlton and Abrahamson (2014), who argue that any variation in correlation coefficients comes from the spectral shape rather than tectonic regime. They state that the correlation coefficients depend on the high-frequency content of ground motions, an effect that could be removed by normalizing the periods by $T_{amp1.5}$, the shortest period when the response spectral value for each ground motion is 1.5 times the PGA. However, after applying the period normalization, the correlations computed in the Mexican data set remain higher than the correlations reported by Abrahamson et al. (2016) and Baker and Jayaram (2008), as shown in Figure 9. Future studies will provide more insight into the actual source and physics of spectral correlations.

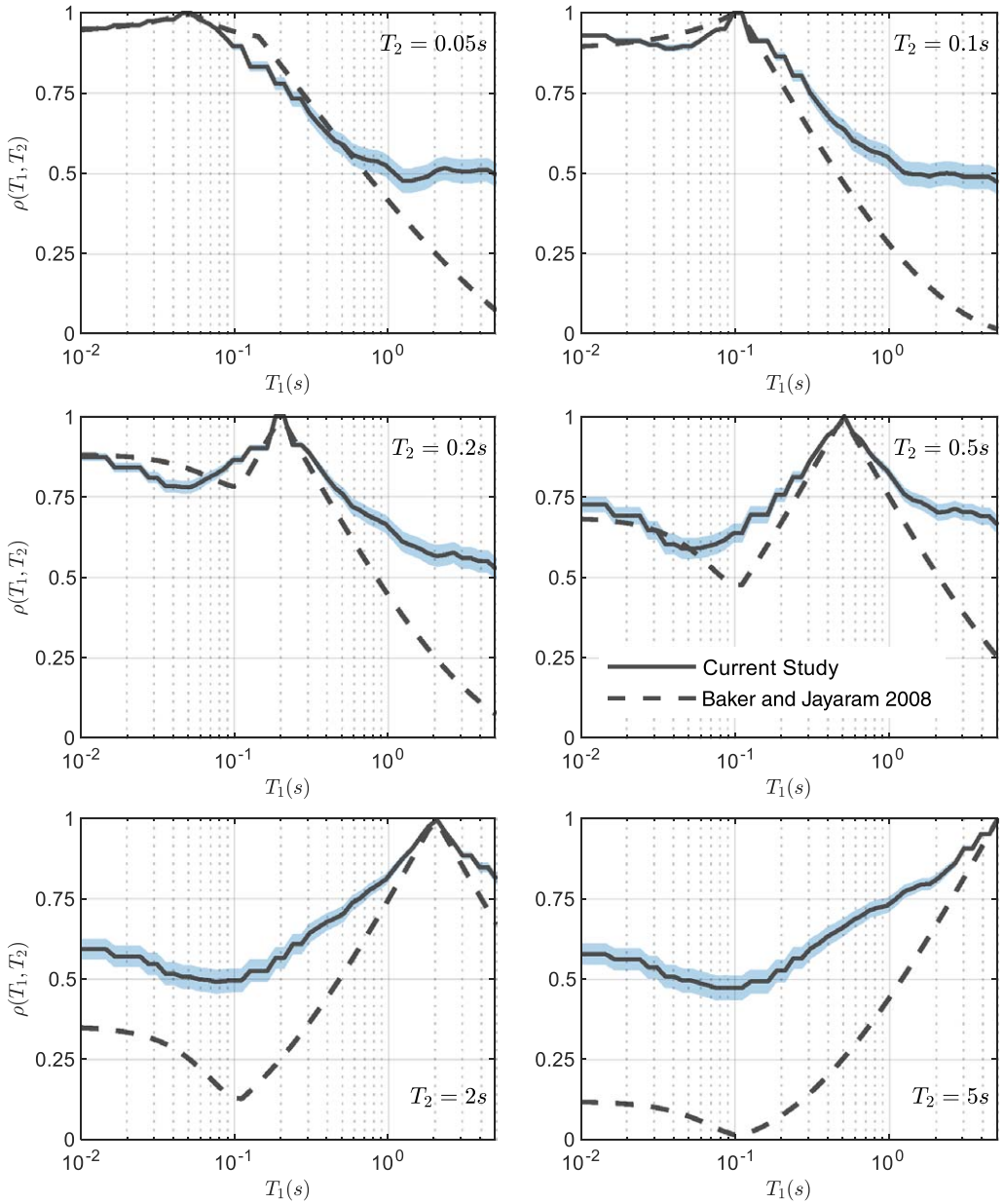

Figure 7. Comparison between correlation models for shallow crustal earthquakes (Baker and Jayaram 2008) and Mexican subduction earthquakes (current study).

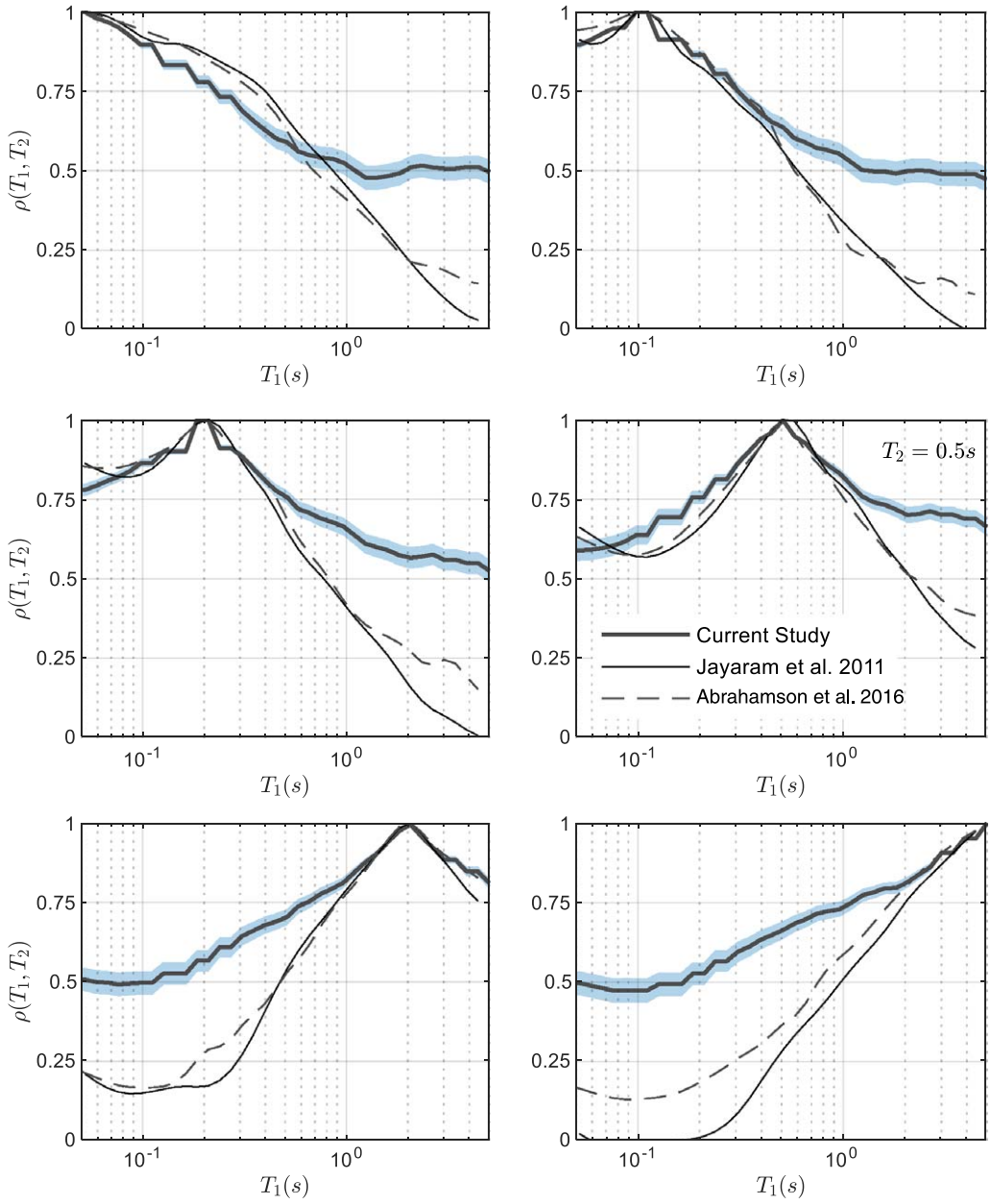

Figure 8. Comparison between correlation models for subduction zones: México (current study), Japan (Jayaram et al. 2011), and Global Data (Abrahamson et al. 2016).

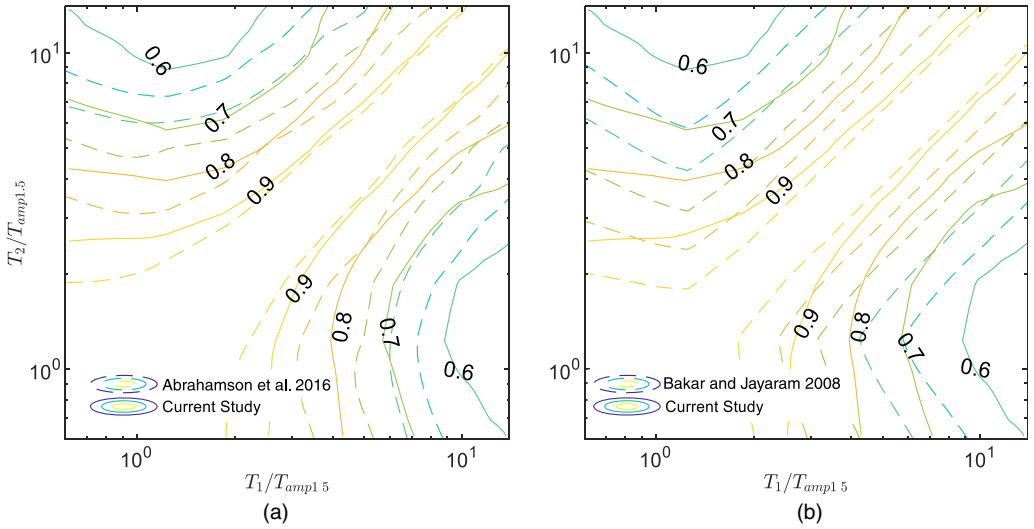

Figure 9. Total residual correlation as a function of normalized periods. Continuous lines represent the Mexican data set with $T_{\text{amp1.5}} = 0.081$ sec.; (a) the dashed lines represent the global data set by Abrahamson et al. (2016), and (b) the dashed lines correspond to the Baker and Jayaram 2008 predictions for shallow crustal earthquakes, both with $T_{\text{amp1.5}} = 0.08$ sec.

CONCLUSIONS

We present a simplified correlation model for total PGV, PGA, and *Sa* residuals at rock sites developed using Mexico's SSN–UNAM strong-motion database. Only records with a site-to-source distance less than 400 km and moment magnitude $5 \leq \text{Mw} \leq 8$ and those recorded at NEHRP Class B sites were considered. A mixed-effect regression model and the García-Soto and Jaimes (2017) attenuation relationship were used to compute between-event and within-event residuals, from which correlations were obtained based on the recommendations by Carton and Abrahamson (2014).

Current results were compared against Baker and Jayaram's (2008) model for shallow crustal earthquakes and two correlation models for subduction interface earthquakes to study the influence of the tectonic regime and the underlying strong-motion data set. Similar to previous studies, the correlation of total residuals is largely controlled by the correlation of within-event residuals; however, it is apparent that *Sa* correlations from Mexican interface earthquakes are consistently higher than Baker and Jayaram's (2008) predictions for crustal earthquakes. Surprisingly, large differences also exist between the correlation model for Mexico and Japan, a result that may be influenced by several factors, such as site heterogeneity, frequency content of ground motions, and style of faulting.

ACKNOWLEDGMENTS

The authors acknowledge the two anonymous reviewers and editor, whose comments and suggestions considerably improved the strength of this article. This research was partially

sponsored by Instituto de Ingeniería at UNAM through the Research Fund R974, Facultad de Ingeniería Civil at Universidad del Desarrollo, the National Research Center for Integrated Natural Disaster Management CONICYT/FONDAP/15110017, and FONDECYT Grant Number 1170836, "SIBER-RISK: SImulation Based Earthquake Risk and Resilience of Interdependent Systems and NetworKs." The authors are grateful for this support. The ground motions used in this study are those used by previous authors whose works are listed in the references (García et al. 2005, García 2006, Arroyo et al. 2010, Hong et al. 2010, García-Soto et al. 2012, García-Soto and Jaimes 2017).

APPENDIX

Please refer to the online version of this manuscript to access the supplementary material provided in the Appendix.

REFERENCES

Abrahamson, N. A., and Silva, W. J., 1997. Empirical response spectral attenuation relations for shallow crustal earthquakes, *Seismological Research Letters* **68**, 94–127.

Abrahamson, N., and Silva, W., 2008. Summary of the Abrahamson & Silva NGA ground-motion relations, *Earthquake Spectra* **24**, 67–97.

Abrahamson, N. A., and Youngs, R. R., 1992. A stable algorithm for regression analyses using the random effects model, *Bulletin of Seismological Society of America* **82**, 505–510.

Abrahamson, N., Gregor, N., and Addo, K., 2016. BC Hydro Ground Motion Prediction Equations for subduction earthquakes, *Earthquake Spectra* **32**, 23–44.

Al Atik, L. A., Abrahamson, N., Bommer, J. J., Scherbaum, F., Cotton, F., and Kuehn, N., 2010. The variability of ground-motion prediction models and its components, *Seismological Research Letters* **81**, 794–801.

Arroyo, D., García, D., Ordaz, M., Mora, M. A., and Singh, S. K., 2010. Strong ground-motion relations for Mexican interplate earthquakes, *Journal of Seismology* **14**, 769–785.

Baker, J. W., 2011. Conditional mean spectrum: Tool for ground-motion selection, *Journal of Structural Engineering* **137**, 322–331.

Baker, J. W., and Bradley, B. A., 2017. Intensity measure correlations observed in the NGA-West2 database, and dependence of correlations on rupture and site parameters, *Earthquake Spectra* **33**, 145–156.

Baker, J. W., and Cornell, C. A., 2006. Correlation of response spectral values for multi-component ground motions, *Bulletin of Seismological Society of America* **96**, 215–227.

Baker, J. W., and Jayaram, N., 2008. Correlation of spectral acceleration values from NGA ground motion models, *Earthquake Spectra* **24**, 299–317.

Bindi, D., Massa, M., Luzi, L., Ameri, G., Pacor, F., Puglia, R., and Augliera, P., 2014. Pan-European ground-motion prediction equations for the average horizontal component of PGA, PGV, and 5%-damped PSA at spectral periods up to 3.0 s using the RESORCE dataset, *Bulletin of Earthquake Engineering* **12**, 391–430.

Boore, D. M., 2005. On pads and filters: Processing strong-ground motion data, *Bulletin of Seismological Society of America* **95**, 745–750.

Boore, D. M., and Atkinson, G. M., 2008. Ground-motion prediction equations for the average horizontal component of PGA, PGV, and 5%-damped PSA at spectral periods between 0.01 s and 10.0 s, *Earthquake Spectra* **24**, 99–138.

Boore, D. M., Watson-Lamprey, J., and Abrahamson, N. A., 2006. Orientation-independent measures of ground motion, *Bulletin of the Seismological Society of America* **96**, 1502–1511.

Building Seismic Safety Council (BSSC) of the National Institute of Building, 2004. *NEHRP Recommended Provisions for Seismic Regulations for New Buildings and Other Structures, FEMA 450*, Federal Emergency Management Agency, Washington, DC.

Campbell, K. W., and Bozorgnia, Y., 2008. NGA ground motion model for the geometric mean horizontal component of PGA, PGV, PGD and 5% damped linear elastic response spectra for periods ranging from 0.01 to 10 s, *Earthquake Spectra* **24**, 139–171.

Carlton, B., and Abrahamson, N., 2014. Issues and approaches for implementing conditional mean spectra in practice, *Bulletin of Seismological Society of America* **104**, 503–512.

Chiou, B. J., and Youngs, R. R., 2008. An NGA model for the average horizontal component of peak ground motion and response spectra, *Earthquake Spectra* **24**, 173–215.

Cimellaro, G. P., 2013. Correlation in spectral accelerations for earthquakes in Europe, *Earthquake Engineering & Structural Dynamics* **42**, 623–633.

Cordova, P. P., Deierlein, G. G., Mehanny, S. S. F., and Cornell, C. A., 2001. Development of a two-parameter seismic intensity measure and probabilistic assessment procedure, in *The Second U.S.–Japan Workshop on Performance-Based Earthquake Engineering Methodology for Reinforced Concrete Building Structures*, Sapporo, Hokkaido, Japan, 187–206.

Daneshvar, P., Bouaanani, N., and Godia, A., 2015. On computation of conditional mean spectrum in eastern Canada, *Journal of Seismology* **19**, 443–467.

García, D., 2006. Estimación de parámetros del movimiento fuerte del suelo para terremotos interplaca e intraslab en México central, Ph.D. Thesis, Faculty of Physical Sciences, The Complutense University of Madrid, Madrid, Spain (in Spanish).

García, D., Singh, S. K., Herráiz, M., Ordaz, M., and Pacheco, F., 2005. Inslab earthquakes of Central Mexico: Peak ground-motion parameters and response spectra, *Bulletin of Seismological Society of America* **95**, 2272–2282.

García-Soto, A. D., Hong, H. P., and Gómez, R., 2012. Effect of the orientation of records on displacement ductility demand, *Canadian Journal of Civil Engineering* **39**, 362–373.

García-Soto, D., and Jaimes, M. A., 2017. Ground-motion prediction model for vertical response spectra from Mexican interplate earthquakes, *Bulletin of Seismological Society of America* **107**, 887–900.

Goda, K., and Atkinson, G. M., 2009. Probabilistic characterization of spatially correlated response spectra for earthquakes in Japan, *Bulletin of Seismological Society of America* **99**, 3003–3020.

Hong, H. P., García-Soto, A. D., and Gómez, R., 2010. Impact of different earthquake types on the statistics of ductility demand, *Journal of Structural Engineering* **136**, 770–780.

Huo, J. R., 1989. Study on the Attenuation Laws of Strong Earthquake Ground Motion Near the Source, Ph.D. Thesis, Institute of Engineering Mechanics, China Earthquake Administration, Harbin, China (in Chinese with English abstract).

Inoue, T., and Cornell, C. A., 1990. *Seismic Hazard Analysis of Multi-Degree-of-Freedom Structures, RMS-8*, Reliability of Marine Structures Program, Stanford, CA.

Jayaram, N., Baker, J. W., Okano, H., Ishida, H., McCann, M. W., and Mihara, Y., 2011. Correlation of response spectral values in Japanese ground motions, *Earthquakes and Structures* **2**, 357–376.

Ji, K., Bouaanani, N., Wen, R., and Ren, Y., 2017. Correlation of spectral accelerations for earthquakes in China, *Bulletin of Seismological Society of America* **107**, 1213–1226.

Joyner, W. B, and Boore, D. M., 1982. *Estimation of Response-Spectral Values as Functions of Magnitude, Distance, and Site Conditions, USGS Open File Report 82-881*, Reston, VA.

Kanno, T., Narita, A., Morikawa, N., Fujiwara, H., and Fukushima, Y., 2006. A new attenuation relation for strong ground motion in Japan based on recorded data, *Bulletin of Seismological Society of America* **96**, 879–897.

Kotha, S. R., Bindi, D., and Cotton, F., 2017. Site-corrected magnitude-and region-dependent correlations of horizontal peak spectral amplitudes, *Earthquake Spectra* **33**, 1415–1432.

Kutner, M. H., Nachtsheim, C., and Neter, J., 2004. *Applied Linear Regression Models*, McGraw-Hill/Irwin, New York, NY.

Lin, T., Harmsen, S. C., Baker, J. W., and Luco, N., 2013. Conditional spectrum computation incorporating multiple causal earthquakes and ground-motion prediction models, *Bulletin of Seismological Society of America* **103**, 1103–1116.

Stafford, P. J., 2017. Interfrequency correlations among Fourier spectral ordinates and implications for stochastic ground-motion simulation, *Bulletin of Seismological Society of America* **107**, 2774–2791.

(Received 9 August 2018; Accepted 12 December 2018)